ISSN 1392–1207. MECHANIKA. 2022 Volume 28(3): 222–229

Vibration Energy Harvesting based on Free Body Moving in Space during Vibro Shock Mode

Egidijus STASYTIS*, Rimvydas GAIDYS, Vytautas DANIULAITIS***, Birutė NARIJAUSKAITĖ******

**Kaunas University of Technology, Studentų g. 56-344, Kaunas, Lithuania, E-mail: egidijus.stasytis@ktu.edu.lt*
***Kaunas University of Technology, Studentų g. 56-344, Kaunas, Lithuania, E-mail: rimvydas.gaidys@ktu.lt*
****Kaunas University of Technology, Studentų g. 56-313b, Kaunas, Lithuania, E-mail: vytautas.daniulaitis@ktu.lt*
*****Kaunas University of Technology, Studentų g. 56-323, Kaunas, Lithuania, E-mail: birute.narijauskaite@ktu.lt*

crossref http://dx.doi.org/10.5755/j02.mech.31034

1. Introduction

Advances in electronics and sensor manufacturing technology steadily reduce power consumption of various devices. Thus, environment energy harvesters become capable of supplying electricity to various devices. The spectrum of energy consumed is shown in Fig. 1. This illustration shows energy demand from nano-, microelectronics to macro-electronic systems. Many of these devices can operate on battery power for extended periods of time. There are cases when devices are installed in places that are difficult for people to reach or working conditions are very arduous. In such cases, replacing the batteries is complicated. Such situations reveal the potential of environment energy harvesters, i.e., due to low power required, reaching μW or mW, they are excellent substitutes for traditional electricity sources.

It is often necessary for devices to work both outdoors and indoors regardless of weather conditions. For this reason, mechanical vibrations and human body movements become attractive sources of energy for small electronics [1, 2].

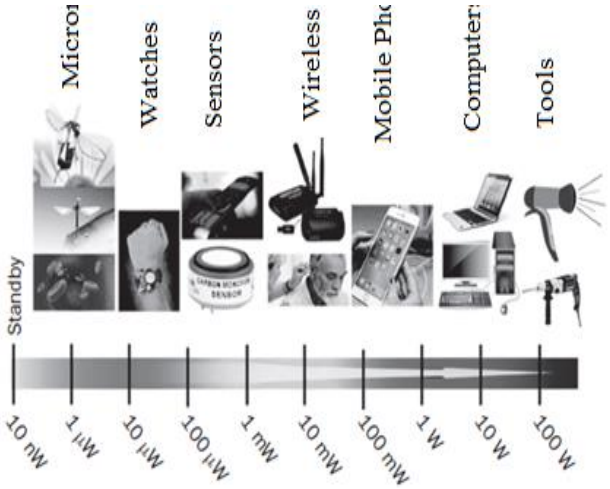

Fig. 1 Energy consumption spectrum of electrical appliances [1]

Potential or kinetic body energy can be converted into electrical, thermal, or other energy employing a variety of materials or devices. The energy of mechanical vibrations can be converted into electrical energy using methods of electromagnetic induction, electrostatic induction, or piezoelectric phenomena [3].

The aim of the research is directed to create mathematical and computational models of the piezoelectric vibration energy harvester (VEH) for a free body moving in space during vibro shock mode. The tasks are to analyse dynamics of the free body moving in space during vibro shock mode; evaluate the simulation and experimentally obtained results; determine the generator output voltage and power dependencies over time.

The COMSOL Multiphysics was used for simulation. MATLAB was used for the mathematical calculations and *Tracker* for analysis of the experimental results.

The piezoelectric phenomenon is characteristic of piezoelectric materials. When a material is deformed, an electric charge occurs on its electrodes. This is called a direct piezoelectric phenomenon. Under the action of an electric field, materials deform, which is the reverse of the piezoelectric phenomenon [4].

Piezoelectric materials can be naturally polarized, such as quartz, or polarized by artificial application of a high-strength static electric field. Ferroelectric ceramics, which are most used in engineering, are currently being polarized in such a way [5].

The efficiency coefficient and power of a piezoelectric generator are highly dependent on the frequency of oscillations since piezoelectric materials generate most electricity at the resonant frequency. S. Roundy [6] determined that the design of generators using the energy of mechanical vibrations must aim to keep the generator operating at the lowest possible eigen frequency, as the output voltage is inversely proportional to the eigen frequency. The oscillation frequencies of most machines during operation reach 100 Hz and above, while human or animal movements are in the range of 1 to 30 Hz [2].

Piezoelectric materials are divided into three groups according to the structural characteristics: single crystals, ceramics, polymers. Piezoelectric materials for generators cannot be selected solely based on the coefficient κ, which determines the relationship between mechanical and electrical coupling. Single crystals and ceramics are effective in converting the energy of mechanical vibrations into electricity ($\kappa = 0.7$). These materials are more sensitive to aging, mechanical impact, they are brittle and withstand lower bending stresses. Therefore, the material chosen for the generating cantilevers was PVDF. Even though the coefficient is only $\kappa = 0.2$ [3], this polymer is insensitive to mechanical impact and aging, it is suitable for impact loads. PVDF is a polymer that is 40 to 50 percent crystalline. The polymer crystal is bimorphic, with two phases (α and β

phases). The β phase is polarized and piezoelectric. To improve the piezoelectric phenomenon, the development of copolymers has begun. Copolymer P (VDF / TrFE) is mainly composed of α-phase PVDF with 90 % crystallinity. Although TrFE is less than half as polarized as PVDF, the high crystallinity of the copolymer results in a high bond coefficient κ in the PVDF polymer [4]. Due to the flexibility of piezoelectric polymers, they are usually produced in the form of a film. This feature allows them to be used in speakers. The performance of PVDF depends on temperature and the method of polarization [7].

Piezoelectric generators that convert the energy of mechanical vibrations into electrical energy are usually of cantilever beam type. When the beam vibrates, large deformations are caused, which the generated voltage depends on. More importantly, the resonant frequency of transverse oscillations of the cantilever is lower than that of other structures, e.g. double support beam. Currently, the most common piezoelectric generators use unimorphic and bimorphic cantilevers (Fig. 2*)*.

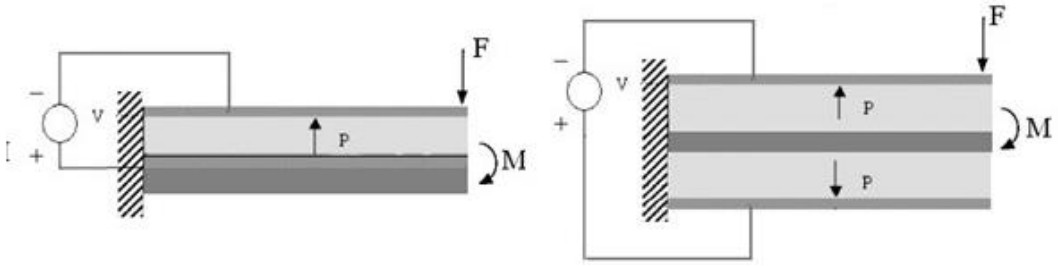

a b

Fig. 2 Unimorphic a) and bimorphic b) piezoelectric generators [8]

The metal cantilever is covered with a thin layer of piezoelectric material on both sides. In this way, a bimorphic structure is obtained, which makes it possible to increase the generated energy. This structure is widely used because it generates twice as much energy [9].

Electromechanical coupling can be described by:

$$\{T\} = \left[c^E\right]\{S\} - \left[d\right]^T \{E\}, \tag{1}$$

$$\{D\} = \left[d\right]\{S\} - \left[\varepsilon^S\right]\{E\}, \tag{2}$$

here: $\{T\} = \{T_{11}\ T_{22}\ T_{33}\ T_{23}\ T_{13}\ T_{12}\}^T$ is stress vector N/m^2; $\{S\} = \{S_{11}\ S_{22}\ S_{33}\ 2S_{23}\ 2S_{13}\ 2S_{12}\}^T$ is strain vector; $\{E\} = \{E_1\ E_2\ E_3\}$ is electric field strength, V/m; $\{D\} = \{D_1\ D_2\ D_3\}$ is electrical induction, C/m^2; $[c^E]$ is mobility matrix, m/N; $[\varepsilon^S]$ is dielectric penetration matrix, F/m; $[d]$ is piezoelectric constant matrix C/N.

2. Modelling and experimental research

The dynamic analysis of the generator is performed by describing the dynamics of the entire generator and the generating system separately. A reduced two-dimensional generator model was chosen for the analysis of dynamics.

2.1. Modelling of free body dynamics in space during vibro shock mode

The generator casing is considered to be a non-deformable rigid body exposed to external forces (Fig. 3).

The air resistance force F_D acts in the opposite direction to the generator speed vector V. As the generator rotates at an angular velocity ω, a force F_L, (a force determined by the Coriolis acceleration) occurs, which is perpendicular to the velocity vector and the axis of rotation. The body is also affected by the force of gravity mg, where m is the sum of the mass m_1 of the generator casing and the inertial mass m_2, and g is the acceleration of the free fall, ϕ is the angle at which the body moves in the plane [10, 11].

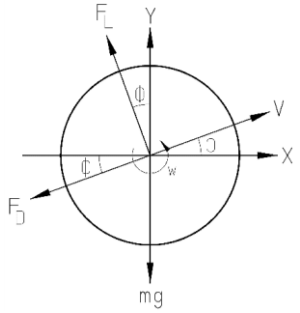

Fig. 3 Forces acting on a body moving and rotating in a 2D space

Generator casing motion equations:

$$m\ddot{x}_1 = -F_D cos\varphi - F_L sin\varphi, \tag{3}$$

$$m\ddot{y}_1 = -F_D sin\varphi + F_L cos\varphi - mg. \tag{4}$$

F_D and F_L forces are described by formulas:

$$F_D = 0.5 C_D \rho A v_1^2, \tag{5}$$

$$F_L = 0.5 C_L \rho A v_1^2, \tag{6}$$

here: ρ is air density, under normal conditions; A is the cross-sectional area of the casing; C_D – air resistance coefficient.

The coefficient C_L is expressed in:

$$C_L = \frac{1}{2 + \frac{v_1}{R\omega}}, \tag{7}$$

here: R is casing radius.

A change is made:

$$\dot{x}_1 = v_1 cos\varphi, \tag{8}$$

$$\dot{y}_1 = v_1 sin\varphi. \tag{9}$$

Then Eqs. (3) and (4) are written as follow:

$$m\ddot{x}_1 = -0.5C_D\rho A\dot{x}_1^2 - 0.5C_L\rho A\dot{y}_1^2, \tag{10}$$

$$m\ddot{y}_1 = -0.5C_D\rho A\dot{y}_1^2 + 0.5C_L\rho A\dot{x}_1^2 - mg. \tag{11}$$

The amount of electricity generated depends on the relative inertial mass motion in respect to the generator casing. The relationship between the generator casing mass m_1 and the vibration-generating inertial mass m_2 is described by the coefficients of spring stiffness k_1 and damping c_1. The mass m_2 is mounted in the center of generator casing. The motion of the system is recorded in the Lagrange equations. Degrees of freedom are depicted in Fig. 4.

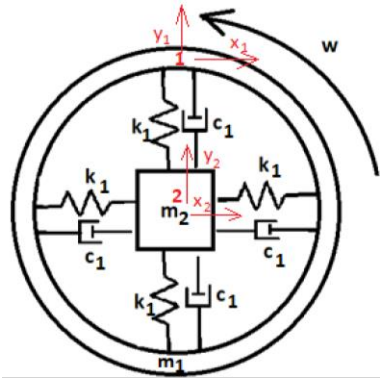

Fig. 4 Computational scheme of the free body

The equations of motion of the inertial mass considering the rotation of the generator casing (Coriolis gyroscopic effects) and the motion are as follow:

$$m_2\ddot{x}_2 + 2k_1x_2 + 2c_1\dot{x}_2 - 2m_2\dot{y}_1\omega - m_2\ddot{x}_1 = 0, \tag{12}$$

$$m_2\ddot{y}_2 + 2k_1y_2 + 2c_1\dot{y}_2 + 2m_2\dot{x}_1\omega - m_2\ddot{y}_1 = 0. \tag{13}$$

The mechanical contact of the generator casing in space is estimated by additional contact relations with coefficients k_2, c_2 and contact force F_C (Fig. 5).

$$F_{cx} = k_2x_2 + c_2\dot{x}_2, \text{ if } x_2 < \Delta, \tag{14}$$

$$F_{cy} = k_2y_2 + c_2\dot{y}_2, \text{ if } y_2 < \Delta, \tag{15}$$

where: Δ is the distance between the generator casing and the obstacle.

So finally, the following equation system for energy harvester (VEH) which moves in space during vibro shock mode is obtained:

$$m_1\ddot{x}_1 + 0.5C_D\rho A\dot{x}_1^2 + 0.5C_L\rho A\dot{y}_1^2 = F_{cx}, \tag{16 a}$$

$$m_1\ddot{y}_1 + 0.5C_D\rho A\dot{y}_1^2 + 0.5C_L\rho A\dot{x}_1^2 - mg = F_{cy}, \tag{16 b}$$

$$m_2\ddot{x}_2 + 2k_1x_2 + 2c_1\dot{x}_2 - 2m_2\dot{y}_1\omega - m_2\ddot{x}_1 = 0, \tag{16 c}$$

$$m_2\ddot{y}_2 + 2k_1y_2 + 2c_1\dot{y}_2 + 2m_2\dot{x}_1\omega - m_2\ddot{y}_1 = 0. \tag{16 d}$$

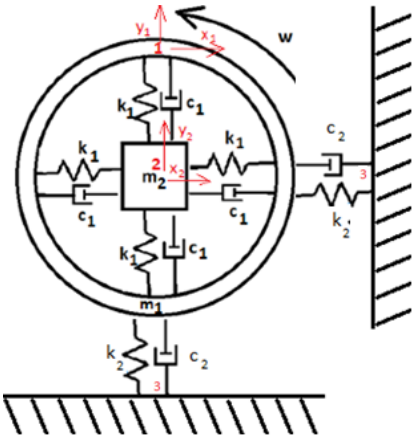

Fig. 5 Computational scheme of the free body contact

Or in matrix form:

$$[M]\{\ddot{q}\} + [C+G]\{\dot{q}\} + [K]\{q\} = \{F_C\}, \tag{17}$$

$$[M] = \begin{bmatrix} m_1 & 0 & 0 & 0 \\ 0 & m_1 & 0 & 0 \\ 0 & 0 & m_2 & 0 \\ 0 & 0 & 0 & m_2 \end{bmatrix}, \tag{18}$$

$$[C] = \begin{bmatrix} 0 & 0 & 0 & 0 \\ 0 & 0 & 0 & 0 \\ 0 & 0 & c_1 & 0 \\ 0 & 0 & 0 & c_1 \end{bmatrix}, \tag{19}$$

$$[K] = \begin{bmatrix} 0 & 0 & 0 & 0 \\ 0 & 0 & 0 & 0 \\ 0 & 0 & k_1 & 0 \\ 0 & 0 & 0 & k_1 \end{bmatrix}, \tag{20}$$

are respectively the mass, damping and stiffness matrices

$$[G] = \begin{bmatrix} 0 & 2m_2\omega & 0 & 0 \\ 2m_2\omega & 0 & 0 & 0 \\ 0 & 0 & 0 & 0 \\ 0 & 0 & 0 & 0 \end{bmatrix}, \tag{21}$$

an asymmetric matrix of gyroscopic forces that links the motion of the generator in both directions. This force is proportional to the inertial mass (m_2).

2.2. Experimental research of the dynamics of vibro shock of the generator

The study of the transient vibration mode of the generator was performed employing experimental equipment, the scheme of which is shown in Fig. 6. The study used a generator *1*, a camera *Huawei Honor* 20 *2*, a base *3*,

a computer *4* with installed *Tracker 5.1.4* software and *Matlab* software.

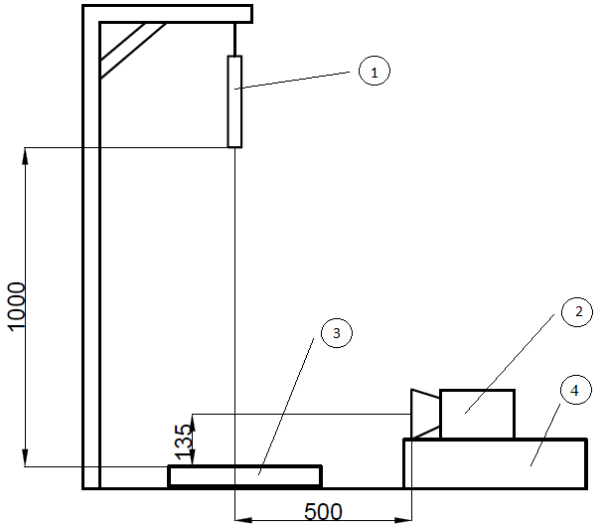

Fig. 6 Experimental scheme: *1* – generator, *2* – camera Huawei *Honor 20*, *3* – base, *4* – computer with software *Tracker 5.1.4* installed

The generator shown in Fig. 7 consists of a rubber ring *1*, four springs *2*, and an inertial mass.

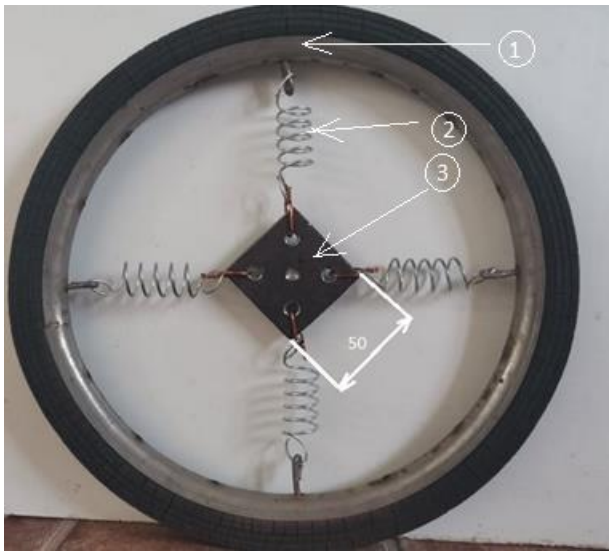

Fig. 7 Generator: *1* – rubber ring, *2* – spring, *3* – inertial mass

The experiment is performed by hanging the generator at a height of 1 m between its lowest point and the base. The concrete block is positioned horizontally to reduce the impact of side effects, the base under the block is leveled with a thin layer of sand. The Huawei *Honor 20* device, which is placed at a distance of 0.5 m from the research object, is used for recording the transition process. The value of the inertial mass (0.1 kg) was chosen to reduce the frequency of resonant oscillations of the system and the possibility to capture the transient dynamic process by the equipment used in the experiment. The Huawei *Honor 20* has a frame rate of 240 frames per second.

When the recording starts, the subject is released from the support connection and falls freely. After contact with the block the damped vibrations induced by the inertia mass caused by the impact starts.

The obtained experimental data of the vibo shock process are analysed with *Tracker 5.1.4* software (Fig. 8 Casing displacements are fixed at point (B) and inertial masses at (A).

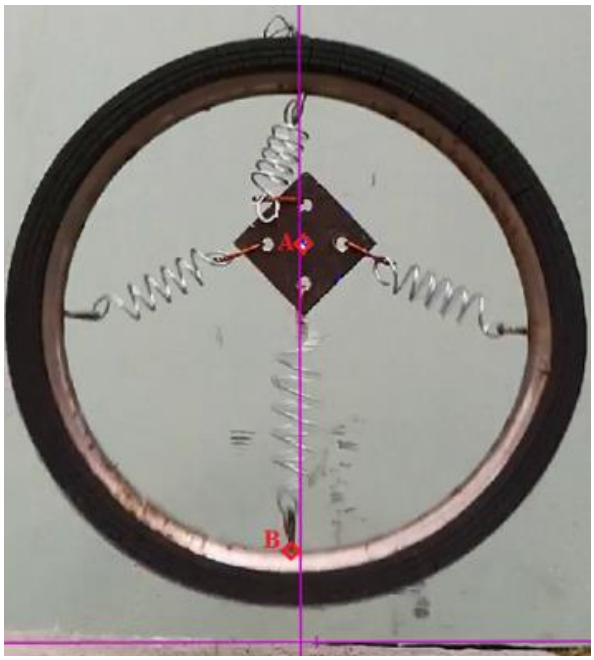

Fig. 8 Experimental record: A is the position of the inertial mass, B is the position of the casing

Experimental results of the transient vibro-shock process are presented in Figs. 9, 10.

The experimental results are processed with *Matlab* software. Subtracting the displacement values of the casing from the values of the vertical displacements of the inertial mass gives the inertial mass displacements with respect to the casing (Fig. 10).

The time interval until the second impact is selected for the study.

The inhibition of the damped free oscillations is determined by the ratio of the homogeneous deviations of the fluctuating mass of two adjacent extremes from the equilibrium position [12]. The value of the logarithmic decrement of the damping oscillations of the experiment is λ = 0.16, whereas damping coefficient is δ = 4.2, and the eigen frequency of the oscillations of the inertial mass is 24.5 Hz.

After performing the simulation, i.e., integrating of the equations of motion (16) the displacements of the generator casing and the inertial mass are obtained. Displacements of the inertial mass with respect to the casing are shown in Fig. 11.

Logarithmic decrement of oscillations is λ = 0.17, damping coefficient is δ = 4.4, eigen frequency of inertial mass oscillations is 25.9 Hz. The relative error between experimental and numerical results is: for eigenfrequency – 5.0 %, for decrement of oscillations - 6.2 % and for damping coefficient – 4.7 %.

The experimental and numerical simulation results of the generator casing are presented in Fig. 13.

The results of modeling and the experiment are well correlated. A slight discrepancy in the results is obtained because the generator casing is described in the model as a rigid body, although in reality it is a deformable body, so its vibrations also occur.

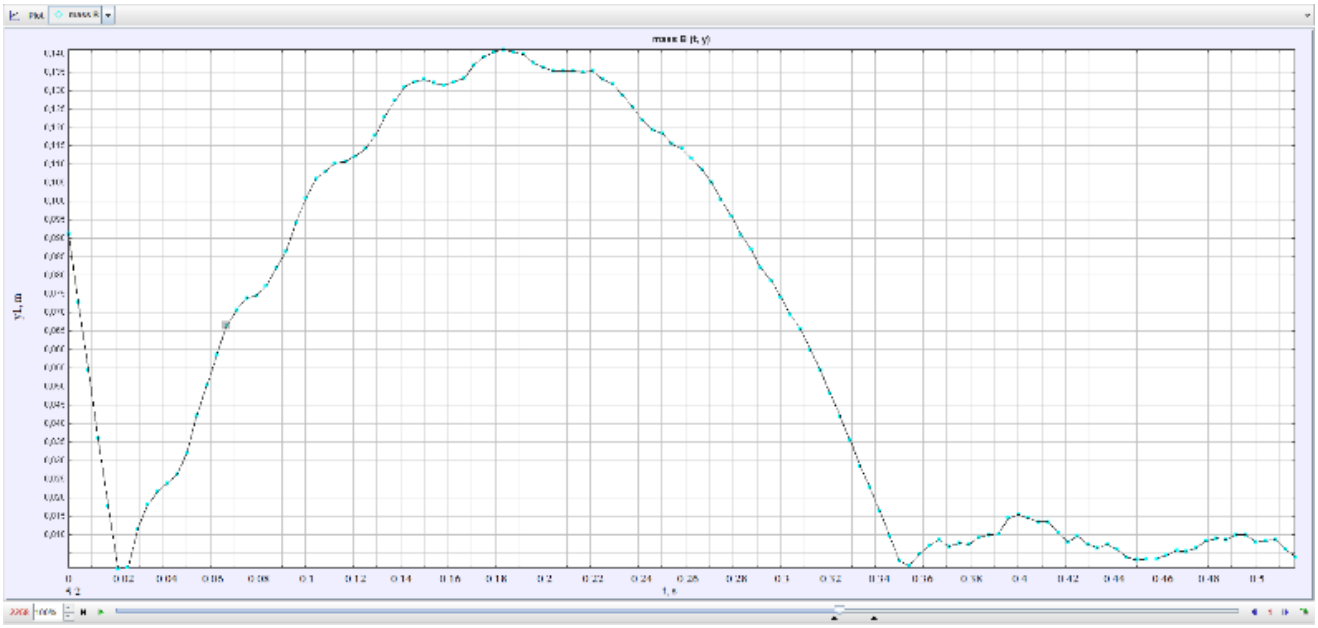

Fig. 9 Displacement of generator casing

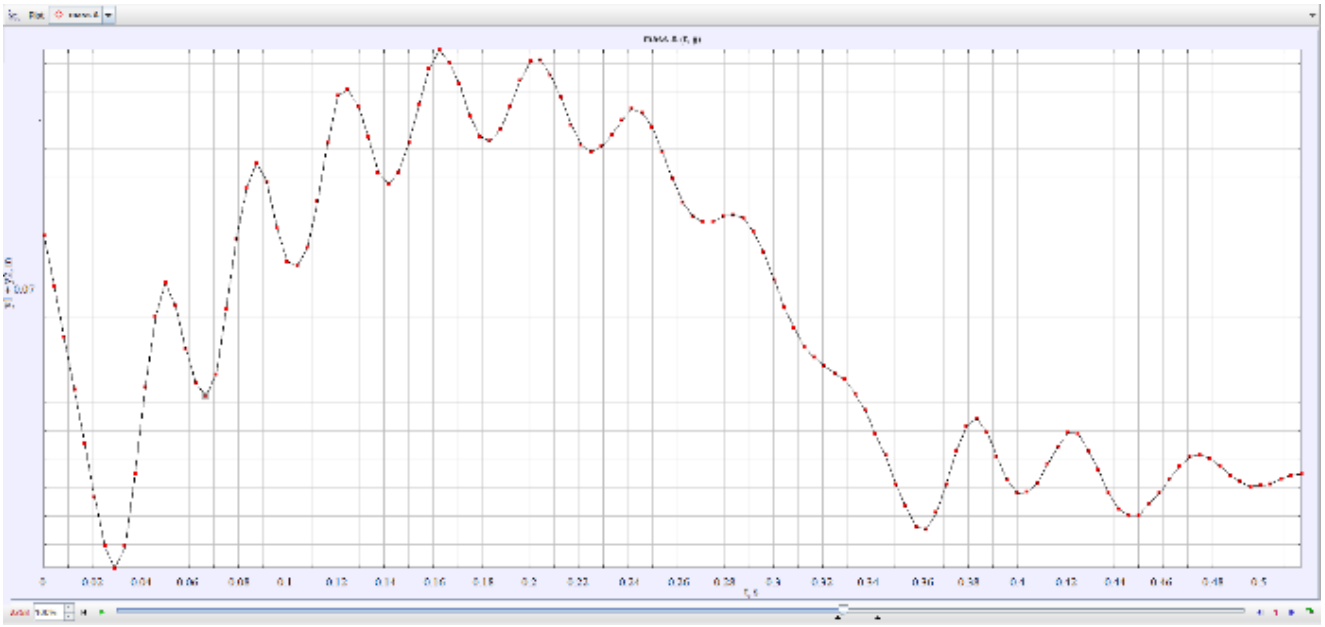

Fig. 10 Displacement of generator inertial mass

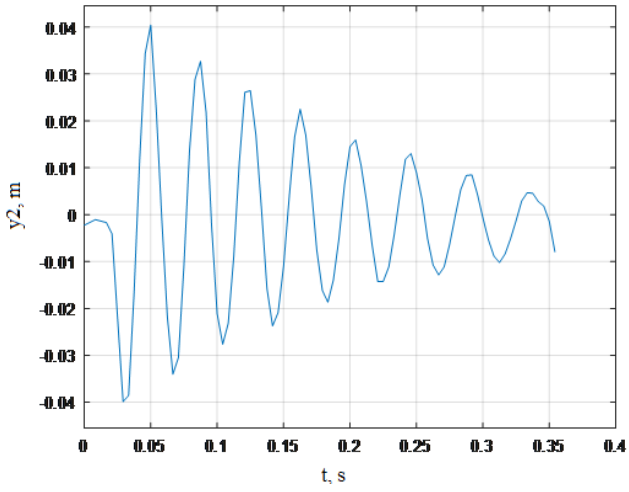

Fig. 11 Experimental results - displacements of the inertial mass in time up to the second impact

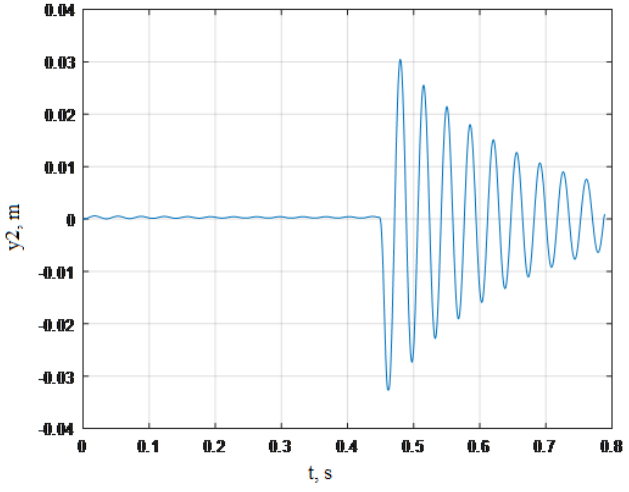

Fig.12 Simulation results - displacements of the inertial mass in time up to the second impact

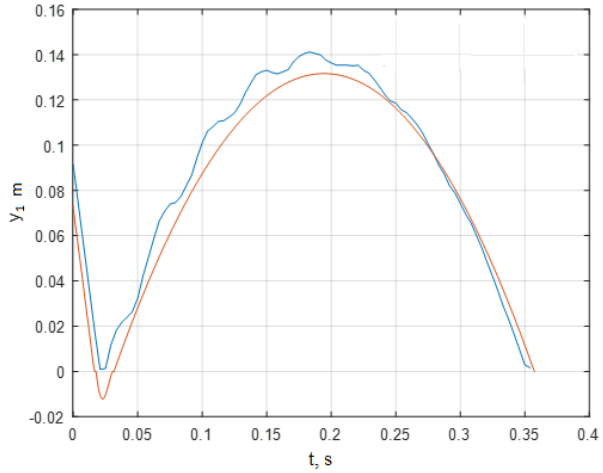

Fig. 13 Generator casing oscillations over time: blue - experimental, red - simulation

3. Modelling the electromechanical coupling of the active element of VEH

The eigen frequency of the oscillations of the inertial mass of the generator tested during the experiment is 24.5 Hz. At low eigen frequency of the inertial mass, it is difficult to select electricity generating elements. Thus, the parameters of the system elements have been changed so as to increase the generator's natural frequency and, with it, the amount of electricity generated. The value of the eigen frequency is 40 Hz, the corresponding parameter values are as follow: inertia mass m_2 = 0.07 kg, spring stiffness k_1 = =2200 N/m. The following initial motion conditions are selected: the generator falls freely vertically from 1.2 m, angular speed is 1rad/s. The simulation was performed, the trajectory of the generator casing is shown in Fig. 13, where two impacts of the generator casing to the ground and bounce are seen. Fig. 14 reveals the oscillations of the inertial mass of the generator, which are particularly induced during the impact of the casing on the ground. As the generator moves and rotates, vibrations caused by the rotation also occur. These oscillations of the inertial mass are further used in the study of piezoelectric elements as the kinematic stimulation of the piezoelectric cantilever.

The piezoelectric cantilever (Fig. 16) consists of five layers: two layers of PVDF polymer *1*, three layers of silver electrodes *2* and two layers of acrylic plastic *3*. The voltage generated during PVDF deformations is discharged by means of silver electrodes. A ground pole is connected to the central electrode, and a terminal for voltage disconnection and connection to load *R* is connected to the external ones. Acrylic plastic serves the purpose of protection against external influences.

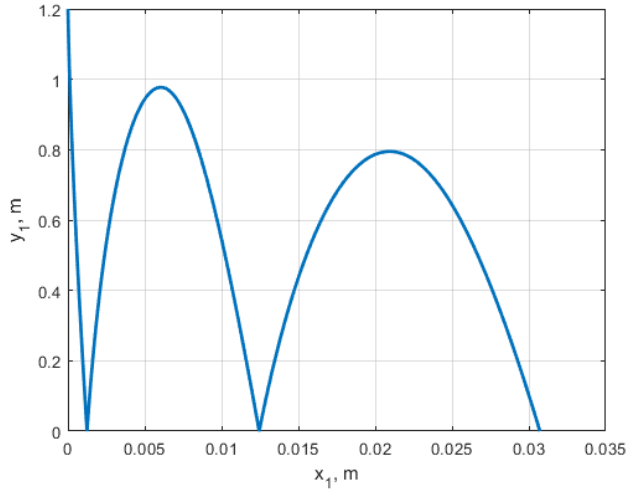

Fig. 14 Generator casing trajectory

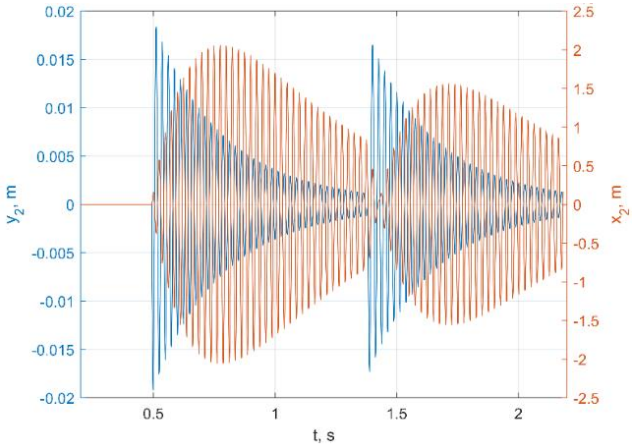

Fig. 15 Oscillations of the inertial mass in time: blue - in the vertical direction, red - in the horizontal direction

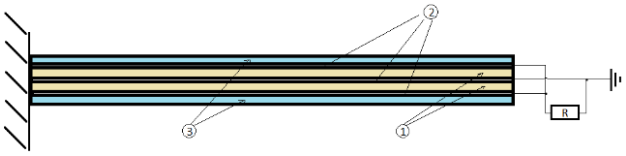

Fig. 16 Scheme of the piezoelectric bimorph

Cantilever dimensions: 16 mm width, 126 μm thickness, 29 mm length. PVDF film thickness – 28 μm, silver electrode – 10 μm, acrylic plastic – 20 μm. In the case of used PVDF, the matrices c^E, d, ε^S are:

$$[c^E]=\begin{bmatrix} 3.8\cdot10^{-9} & 1.9\cdot10^{-9} & 0.9\cdot10^{-9} & 0 & 0 & 0 \\ 1.9\cdot10^{-9} & 3.8\cdot10^{-9} & 0.9\cdot10^{-9} & 0 & 0 & 0 \\ 0.9\cdot10^{-9} & 0.9\cdot10^{-9} & 1.2\cdot10^{-9} & 0 & 0 & 0 \\ 0 & 0 & 0 & 0.7\cdot10^{-9} & 0 & 0 \\ 0 & 0 & 0 & 0 & 0.9\cdot10^{-9} & 0 \\ 0 & 0 & 0 & 0 & 0 & 0.9\cdot10^{-9} \end{bmatrix}, \quad [d]=\begin{bmatrix} 0 & 0 & 0 & 0 & 0 & 0 \\ 0 & 0 & 0 & 0 & 0 & 0 \\ 0.024 & 0.001 & -0.027 & 0 & 0 & 0 \end{bmatrix},$$

$$[\varepsilon^S]=\begin{bmatrix} 7.4 & 0 & 0 \\ 0 & 9.3 & 0 \\ 0 & 0 & 7.6 \end{bmatrix}.$$

The first eigen frequency of the transverse oscillations of the piezoelectric element is 39.19 Hz, for which the determination of the optimal electrical load is performed. The generated electrical power and voltage when the resistance varies in the range of 10^5 – 10^7 Ω are investigated (Fig. 17).

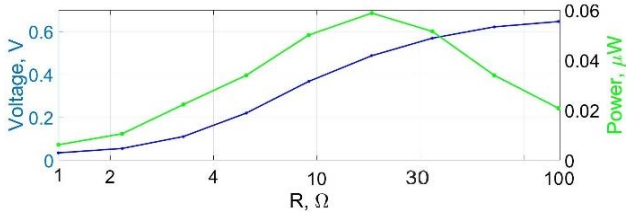

Fig. 17 Relation of generated voltage and output power on electrical load at eigen frequency of 39Hz. Blue – generated voltage, V; green - output power, μW

The graph shows that the maximum power generated is 0.05 μW at a load of about 2 MΩ, so the output power and voltage at a load of 2 MΩ are further investigated, and the harmonic analysed of the active element was done in the interval of 30 – 45 Hz (Fig. 18).

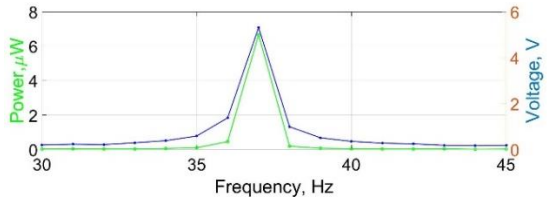

Fig. 18 Relation of generated voltage and output power under load of 2 MΩ. Blue output voltage, V; green – output power μW

The obtained graph reveals that the maximum voltage of 5.25 V and power of 6.75 μW are generated at a frequency of 37 Hz, which is close to the eigen frequency of the active element of 39 Hz.

The simulation of the transient analyse of the generated voltage and power over time is performed. Two piezoelectric elements *1* are attached to the inertial mass *2* (Fig. 19).

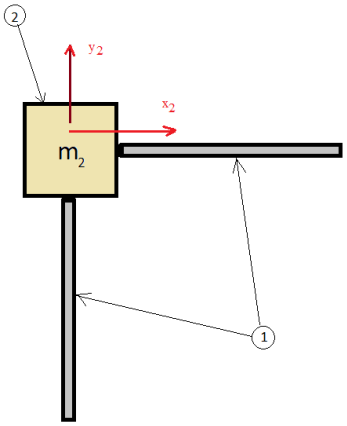

Fig. 19 Generator computational scheme: *1* – piezoelectric elements, *2* – inertial mass m_2

The oscillations of the inertial mass m_2 are presented in Fig. 15. At this stage of the study, these oscillations are the kinematic excitation of the piezoelectric element provided by the generator in Fig. 19 at its point of attachment to the mass m_2. The output voltage and power of each piezoelectric element are examined separately.

Table 1

Test results of piezoelectric element output voltage and power

Examined cantilever	Generated voltage $U(t)$, V	Output power $P(t)$, μW
	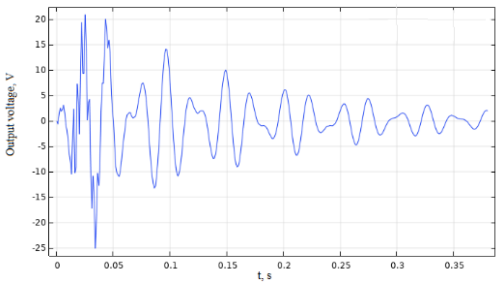	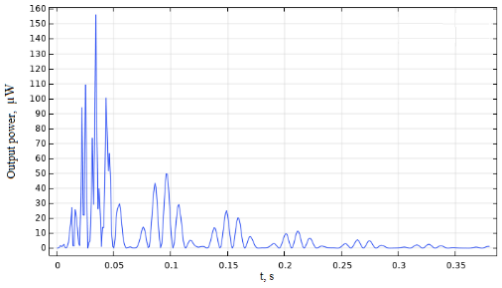
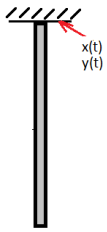	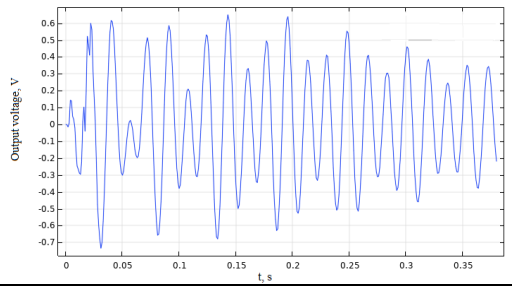	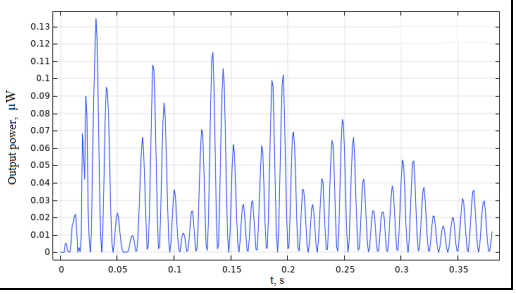

Transient simulation of voltage and power is performed using the *Comsol Multiphysics* system. The results of the study are presented in Table 1.

The obtained results show that the maximum output voltage of the horizontal cantilever is 20 V, the maximum power is 155 μW, the maximum voltage of the vertical cantilever is 0.65 V, the maximum power is 0.135 μW. The vertical cantilever generates very little electricity because its total amplitude value of the transverse oscillations is only 2 10^{-3} m due to the initial conditions used in the study: initial speed of the generator casing, acceleration, angular frequency.

A conception of the piezoelectric harvester is presented in Fig. 20.

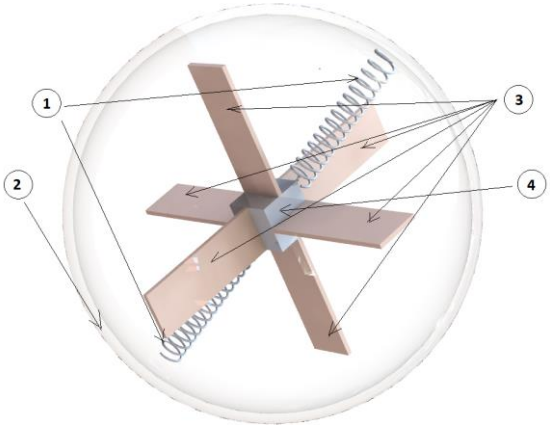

Fig. 20 Conceptual design of the harvester: *1* – springs, *2* – body, *3* – piezoelectric beams, *4* – holder

Harvester consist of six piezoelectric bimorphic beams connected at a holder. A holder is connected with body by springs in all planes (in Fig. 20 only two presented). Electronic equipment can be placed in the holder and it can be as inertial mass.

4. Conclusions

A reduced two-dimensional generator model was created for the analysis of the dynamics of the vibration energy harvester (VEH) for a free body moving in space during vibro shock mode. The mathematical model was created. Analysis of experimental and simulation results is performed. Comparison of generator eigen frequencies - experimental – 24.5 Hz, simulated – 25.9 Hz. The experimental logarithmic decrement value is λ = 0.16 and the damping coefficient is δ = 4.2; simulation logarithmic decrement is λ = 0.17, damping coefficient is δ = 4.4. The maximum output voltage value of the horizontal piezoelectric cantilever is 20 V, the maximum power output value is 155 μW. The maximum output voltage value of the vertical cantilever is 0.65 V, and the maximum power value is 0.135 μW. In horizontal position, the piezoelectric element generates significantly more electricity than in vertical one. To increase the output power and voltage of the vertical cantilever, the angular frequency of the generator must be increased.

References

1. **Bandyopadhyay, S.** 2019. Fabrication and Application of Nanomaterials. Applications in Energy Harvesting, Chapter. McGraw-Hill Education.
2. **Li, H.; Tian C.; Deng, Z. D.** 2014. Energy harvesting from low frequency applications using piezoelectric materials Applied Physics Reviews 1: 04130. https://doi.org/10.1063/1.4900845.
3. **Spies, P.; Pollak, M.; Mateu, L.** 2015. Handbook of Energy Harvesting Power Supplies and Applications CRC Press.
4. **Caliò, R.; Rongala, U. B.; Camboni, D; Milazzo, M.; Stefanini, C.; Petris, G.; Oddo, C. M.** 2014. Piezoelectric Energy Harvesting Solutions. https://doi.org/10.3390/s140304755.
5. **Uchino, K.** 1997. Piezoelectric Actuators and Ultrasonic Motors, Kluwer Academic Publishers, MA.
6. **Roundy, S.; Leland, E.S.; Baker, J.; Carleton, E.; Reilly, E.; Lai, E.; Otis, B.; Rabaey, J.M.; Wright, P.K.**; Sundararajan, V. 2005. Improving power output for vibration-based energy scavengers. https://doi.org/10.1109/MPRV.2005.
7. **Sadegh, A. M., Worek, W. M.** 2018. Marks' Standard Handbook for Mechanical Engineers, 12th Edition.
8. Unimorfinė ir bimorfinė gembės [picture] [accessed 09 Jun. 2019]. Available from Internet: https://www.jvejournals.com/article/14595.
9. **Grzybek, D.** 2013. Piezoelectric generators: materials and structures, Pomiary Automatyka Robotyka 10: 123-129.
10. Piezo Ceramic Bimorph 40×10×0.5mm [accessed 02 Jan. 2020]. Available from Internet: https://www.steminc.com/PZT/en/piezo-ceramic-bimorph-40x10x05mm-2-khz.
11. **Penner, A. R.** 2001. The physics of golf: The optimum loft of a driver. American Journal of Physics 69. https://doi.org/10.1119/1.1344164.
12. **Žiliukas, P.; Barauskas, R.** 2008. Mechaniniai virpesiai. Vilnius: Pedagoginio universiteto leidykla.

E. Stasytis, R. Gaidys, V. Daniulaitis, B. Narijauskaitė

VIBRATION ENERGY HARVESTER (VEH) FOR A FREE BODY MOVING IN SPACE AT VIBRO SHOCK MODE

S u m m a r y

The type of the generator was chosen to be piezoelectric because it is most widely used to capture the energy of mechanical vibrations and convert it into electricity. A 2D generator model was chosen for the analysis of the dynamics of the energy harvester (VEH) for a free body moving in space during vibro shock mode. The computational schemes of the model are presented. A mathematical model describing the dynamics is developed: generator casing, inertial mass, nonlinear contact/impact. The mathematical model is implemented by the Runge-Kutta numerical method in the *Matlab* system. Analysis of experimental and modeling results is performed: comparison of generator eigen frequencies, the logarithmic decrement and the damping coefficient – the error is in range of 5%. This generator can be used to collect mechanical energy of water waves, wind, human movements, and other environmental factors in the presence of the body's free movement trajectory in space.

Keywords: piezoelectric transducers, modelling and simulation, piezoelectric transduction mechanism, vibration energy harvester, vibro shock.

Received March 29, 2022
Accepted June 14, 2022